Spacecraft Attitude Dynamics
Academic Year 2022/2023

Project group **n. 45**
Project **n. 140**

Surname:	**Name:**	**ID:**	**Bachelor:**
Boni	Andrea	10493572	Ingegneria Aerospaziale - Milano
Lo Iacono	Marco	10092136	Ingegneria Aerospaziale - Milano
Luciardello Lecardi	Matteo	10572870	Ingegneria Aerospaziale - Milano
Ricci*	Lorenzo	10937610	Ingegneria Aerospaziale - Pisa

*withdrew for medical reasons in late October

Contents

List of Figures

List of Tables

1 Introduction

This project aims to develop a full simulation of the attitude dynamics, determination and control of a spacecraft. It will present the dynamics of a satellite in a typical operational environment, how attitude is represented, how it is determined autonomously by various sensors and controlled by various actuators. In table 1 the mandatory project specifications are shown.

Platform	**Attitude parameter**	**Mandatory sensor**	**Actuators**
CubeSAT 6U	Direction cosines	Gyroscopes	Constant thrust jets

Table 1: Project n. 140 specifications

2 Orbit

It's assumed the spacecraft is launched from Kourou ESA spaceport (French Guiana). By referring to the Ariane 6 Launcher's User Manual is selected an orbit compatible with a commercial low-cost launcher service: orbit inclination 6 degree; pericenter altitude 400 km; apocenter altitude 600 km. Because of low-inclination, equatorial Earth radius 6378.137 km is assumed as altitude reference. Eccentricity and semi-major axis are computed accordingly by simple geometric relationships, while the remaining keplerian elements are null (table 2). The angle

a	e	Δi	$\theta(t_0)$	Ω	$\bar{\omega}$
6878.1 km	0.014539	6.0 deg	0.0 deg	0.0 deg	0.0 deg

Table 2: Keplerian elements

$\theta(t)$ is provided by means of numerical integration.

$$\dot{\theta} = \frac{(1 + e\ \cos\theta)^2}{\sqrt{(1-e^2)^3}} \sqrt{\frac{\mu}{r(\theta)^3}} \qquad r(\theta) = \frac{a(1-e^2)}{1 + e\ cos\theta} \tag{1}$$

The orbit period T is about 1 hour, 34 minutes, 37 seconds.

$$T = 2\pi \sqrt{\frac{a^3}{\mu}} = 5677.061 \text{ s} \tag{2}$$

The initial time t_0 is fixed at 12:44 UTC of 22 september 2024. Since it's the autumnal equinox, the Sun right ascension $\alpha_S(t_0)$ and declination $\delta_S(t_0)$ are known, as well as the right ascension of Greenwich meridian $\alpha_G(t_0)$.

3 Reference frames

First, recall the rotation matrices $R_i(\alpha)$.

$$R_1(\alpha) = \begin{bmatrix} 1 & 0 & 0 \\ 0 & \cos\alpha & \sin\alpha \\ 0 & \sin\alpha & \cos\alpha \end{bmatrix} \quad R_2(\alpha) = \begin{bmatrix} \cos\alpha & 0 & -\sin\alpha \\ 0 & 1 & 0 \\ \sin\alpha & 0 & \cos\alpha \end{bmatrix} \quad R_3(\alpha) = \begin{bmatrix} \cos\alpha & \sin\alpha & 0 \\ -\sin\alpha & \cos\alpha & 0 \\ 0 & 0 & 1 \end{bmatrix}$$

In order to describe the spacecraft attitude dynamics at least three reference frames must be provided:

ECI: It's the Earth Centred Inertial reference frame. It's used to describe spacecraft and celestial bodies orbital mechanics, as well as to evaluate the spacecraft space environment e.g. Solar Radiation Pressure (SRP) or eclipse occurrences. The ECI x-axis is the vernal axis, the z-axis is normal to equatorial plane, the y-axis is obtained accordingly with the right-hand rule.

BODY: It's the attitude reference frame. It's provided by spacecraft principal inertia axes and it's centred in the spacecraft centre of mass (CoM). In this project is assumed that the CoM is not coincident with the spacecraft geometric centre. Referring to BODY frame is the best way to write the attitude dynamics Euler equations and the cosine matrix $A_{B/N}$.

GCS: The Geographic Coordinate System coordinates are longitude, latitude and altitude. GCS is related to Earth-Centred Earth-Fixed (**ECEF**) reference frame, where the z-axis points North Pole while x-y axis rotate with the planet s.t. the Greenwich meridian belongs to +x. Those frames are required to compute the Earth magnetic field at spacecraft longitude and latitude.

Then, the perifocal frame is introduced to describe the spacecraft orbital mechanics:

Perifocal: It the orbit keplerian frame s.t. the x-axis is directed to pericenter, the y-axis aligned to semi-rectum, the z-axis normal to orbit plane. Fixed the orbit, note that the relative position btw ECI and perifocal frame is a constant cosine matrix.

$$A_{P/N} = R_3(\bar{\omega})R_1(i)R_3(\Omega) \qquad \text{from ECI to perifocal} \tag{3}$$

LVLH: It's the Local-Vertical Local-Horizontal rotating frame. The z-axis is aligned to the spacecraft-radius versor $\hat{\mathbf{r}}$, the y-axis is normal to orbit plane, the x-axis follows the right-hand rule, e.g. the spacecraft is Earth pointing when the $-$z axis of the BODY frame is direct as the $-$z axis of the LVLH frame. In addiction, it's assumed that the spacecraft attitude requirements include Earth pointing and Sun pointing coming by TELECOM and POWER subsystems.

$$A_{L/N} = A_{L/P}A_{P/N} \qquad \text{from ECI to LVLH} \tag{4}$$

where:

$$A_{L/P} = R_2(\pi/2)\ R_1(\pi/2)\ R_3(\theta) \qquad \text{from perifocal to LVLH}$$

SUN: It's defined such that his z-axis is aligned to sun-radius versor $\hat{\mathbf{r}}_\mathbf{S}$, the y-axis is normal to orbit plane, the x-axis follows the right-hand rule, e.g. the spacecraft is Sun pointing when the +z axis of the BODY frame is directed as the +z axis of the Sun frame.

$$A_{S/N} = [\mathbf{j}_S \times \hat{\mathbf{r}}_S;\ \mathbf{j}_S;\ \hat{\mathbf{r}}_S] \qquad \text{from ECI to SUN} \tag{5}$$

where:

- $\mathbf{j}_S = A_{L/N}^T[0,1,0]^T$
- $\hat{\mathbf{r}}_S$ is the Sun versor in ECI coordinates

Assuming circular Earth orbit model, since t_0 is the vernal equinox:

$$\mathbf{r}_S = R_1^T(\varepsilon)R_3^T(n_S\, t)[1\text{AU},\ 0,\ 0]^T$$

where:

- $n_S = \dfrac{2\pi}{T_{year}}$
- $T_{year} = 365.2563194$ days

(2)

Last but not least, in the spacecraft every device has its own reference frame. In this project all of them are described with respect to the BODY frame. The Star Sensor reference frame is presented in section 5.2, and the actuators placement and orientation are presented in section 6.1.

4 Spacecraft model

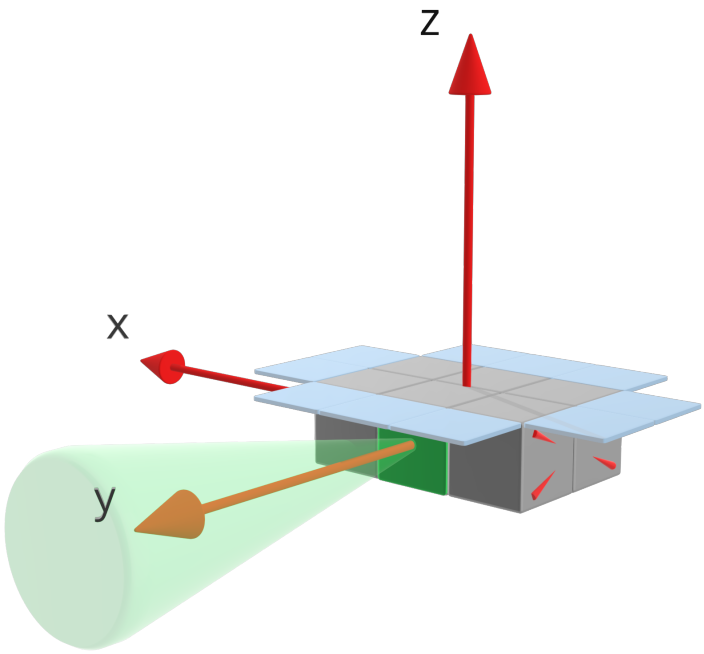

Figure 1: Spacecraft representation

In the present project, the spacecraft is a 6U CubeSAT. A CubeSAT is a type of miniaturised satellite built with standard cubic units of dimensions 10 cm × 10 cm × 10 cm, and mass not exceeding 1.33 kg. The preliminary design must be conservative, hence a mass budget M of 8 kg is assumed.
The 6 units of the CubeSAT are arranged to make a 3U x 2U x 1U spacecraft, Therefore, the length of the spacecraft L_x is 0.3 m, the width L_y is 0.2 m and the height L_z is 0.1 m
Inertia determination follows, that is:

$$I_x = M\frac{L_y^2 + L_z^2}{12} = 0.033333\ kg\ m^2 \qquad \text{minor axis} \tag{3}$$

$$I_y = M\frac{L_x^2 + L_z^2}{12} = 0.066667\ kg\ m^2 \qquad \text{intermediate axis} \tag{4}$$

$$I_z = M\frac{L_x^2 + L_y^2}{12} = 0.086667\ kg\ m^2 \qquad \text{major axis} \tag{5}$$

Remarks:

- Axes of inertia are considered to be translated but not rotated with respect to the geometric axes. The CoM is arbitrary located at coordinates $[0.015, 0.015, 0.015]^T\ m$.
- All additional contributions are nested in the main body mass budget.

To evaluate the total exposed surface, solar panels (SP) must be taken into account, which will be deployed during operations and sized according to EPS demands. Standard solar panel power performance provides about 2.3 W/dm^2 [1], so in order to guarantee a power delivery of at least 40 W, which is reasonable for a 6U CubeSAT, the panel surface area must be greater or equal to about 18 dm^2.

All of this is summarized in table 3, along with orientations, positions and other physical properties.

Identifier	**Orientation**	**Surface** $[m^2]$	**Position**	$\boldsymbol{\rho_s}$	$\boldsymbol{\rho_d}$
A_x^+	$[+1, 0, 0]$	0.02	$[+L_x/2, 0, 0]$	0.5	0.1
A_y^+	$[0, +1, 0]$	0.03	$[0, +L_y/2, 0]$	0.5	0.1
A_z^+	$[0, 0, +1]$	0.06	$[0, 0, +L_z/2]$	0.5	0.1
A_x^-	$[-1, 0, 0]$	0.02	$[-L_x/2, 0, 0]$	0.5	0.1
A_y^-	$[0, -1, 0]$	0.03	$[0, -L_y/2, 0]$	0.5	0.1
A_z^-	$[0, 0, -1]$	0.06	$[0, 0, -L_z/2]$	0.5	0.1
A_{sp}^+	$[0, 0, +1]$	0.10	$[0, 0, +L_z/2]$	0.8	0.1
A_{sp}^-	$[0, 0, -1]$	0.10	$[0, 0, +L_z/2]$	0.8	0.1

Table 3: Spacecraft surfaces

Aerodynamically the spacecraft can be considered as a bluff body, which is always going to generate a turbulent regime in LEO. Therefore a drag coefficient c_d of 2.10 is chosen, picked from a plausible range of 2.05 - 2.20 for this aerodynamic configuration.

Finally, an internal current flow m is present within the spacecraft. According to NASA/SP-8018 when the magnetic torque is dominant the magnitude of m must not be greater than $10^{-3}\ A\ m^2/kg$. Since the CubeSAT is in LEO orbit, it's expected that the magnetic field of the Earth will play a significant role meaning that the higher order terms can't be neglected. Accordingly, the average internal flow m is set to:

$$\mathbf{m} = [0.0015, 0.0077, 0.0015]^T\ A\ m^2 \tag{6}$$

A random contribution is added to $\mathbf{m}$, simulating on-board activity.

5 Sensors

The attitude is determined by making use of two different devices: a gyroscope, and a Star Sensor. The Star Sensor was added because the recovered attitude coming from the gyroscope alone was not accurate enough to allow for proper satellite slew and pointing maneuvers.

5.1 Gyroscope

The gyroscope specifications have been recovered from the Safran Sensing Technologies Norway website[2]:

[1] ISIS CubeSAT Solar Panels: `https://www.CubeSATshop.com/product/single-CubeSAT-solar-panels/`

[2] STIM300 Inertial Measurement Unit: `https://www.sensonor.com/products/inertial-measurement-units/stim300/`

Sample rate	Angular random walk	Bias instability	Size	Weight
up to 2000 Hz	0.15 $\frac{deg}{\sqrt{h}}$	0.30 $\frac{deg}{h}$	45 × 39 × 22 mm	55 g

Table 4: Gyroscope specifications.

The gyroscope has been modelled as:

$$\boldsymbol{\omega}_{gyro} = \boldsymbol{\omega} + \mathbf{n} + \mathbf{b} \tag{7}$$

where:

- $\boldsymbol{\omega}$ is the real angular velocity
- $\mathbf{n}$ is a white noise with variance equal to ARW$/\sqrt{t_s}$, where t_s is the sampling time of the gyroscope
- $\mathbf{b}$ is another white noise with variance equal to RRW$/\sqrt{t_s}$, integrated in time from starting conditions $\mathbf{b}(0) = [1, 1, 1]\,\frac{deg}{h}$

5.2 Star Sensor

The Star Sensor has been modelled in a more complex way. First of all, the boresight of the sensor is oriented as the as the Y axis. To pass from the SENSOR frame to the BODY frame a negative 90 degrees rotation around the Z axis is required, which is embodied in the rotation matrix $A_{B/S}$.

$$A_{B/S} = \begin{bmatrix} 0 & +1 & 0 \\ -1 & 0 & 0 \\ 0 & 0 & +1 \end{bmatrix} \tag{8}$$

Then, the star sensor specifications have been retrieved from Terma's website[3]:

Sample rate	Field of view	Accuracy bias	Size	Weight
up to 10 Hz	circular, 20 deg	0.0027778 deg	100 × 100 × 40 mm	450 + 310 g

Table 5: Star sensor specifications.

The model does not make use of a star catalogue, but instead generates 3 random stars within the field of view of the star sensor. These stars are generated via a function which outputs a uniformly generated value for 2 different angles α_i and β_i, with $i = 1, 2, 3$. The first angle is $\alpha_i \in \left[0, \frac{\theta_{FoV}}{2}\right]$, which is an elevation angle that has a 0 value when the i-th star coincides with the pointing axis of the Star Sensor, which is the y axis of the spacecraft. The second angle is $\beta_i \in [0, 2\pi]$, which is the angle between the projection of the star on the normal plane x-z and the x axis of the spacecraft. The position of the star is then written as:

$$\mathbf{v}_i^S = [\cos\alpha_i,\ -\sin\alpha_i \cos\beta_i,\ \sin\alpha_i \sin\beta_i]^T \tag{9}$$

[3]STIM300 Inertial Measurement Unit: `https://www.terma.com/media/pokirm23/2-pager-_t1-star-tracker.pdf`

which can be considered as the measurements coming from a star catalogue. This vector has then to be rotated into the inertial frame, as:

$$\mathbf{v}_i^N = A_{B/N}^T A_{B/S} \mathbf{v}_i^S \tag{10}$$

where each $bias_{SS}$ is a white noise with variance equal to the bias of the Star Sensor, $A_{B/N}^T$ is the BODY to INERTIAL matrix and $A_{B/S}$ is the SENSOR to BODY matrix. The measurement vector s_i^B is calculated as the catalogue measurement, pre-multiplied by an error matrix which includes the bias of the Star Sensor, and then rotated into BODY frame:

$$\mathbf{s}_i^B = \left[A_{B/S} A_{err} \mathbf{v}_i^S\right]^T \text{ with } A_{err} = \begin{bmatrix} 1 & -bias_{SS,x} & bias_{SS,y} \\ bias_{SS,x} & 1 & -bias_{SS,z} \\ -bias_{SS,y} & bias_{SS,z} & 1 \end{bmatrix} \tag{11}$$

Therefore, the output of the Star Sensor will be the exact "catalogue" vector of each star in INERTIAL frame $\mathbf{v}_i^N$, and the "measured" vector of the star in BODY frame $\mathbf{s}_i^B$.

6 Actuators

Two types of actuator have been used: constant jet thrusters, which were the mandatory actuators required for the project, and reaction wheels, which will be used in order to reduce the required propellant mass, as it would be infeasible to have a long lasting mission to strictly make use of jet thrusters, because the fuel consumption could never be satisfied on a CubeSAT.

6.1 Constant jet thrusters

Each constant thruster jet has properties which have been taken from the Micro Aerospace Solutions database[4], as shown in table 6:

Thrust (N)	0.005
Specific Impulse (s)	150
Propellant	NOx/Ethylene
Inlet Pressure (Pa)	350,000
Min. Impulse bit (N s)	1.7×10^{-4}
Weight (kg)	0.010
Exit diameter (mm)	3.81
Pulse life	$>$ 100,000
Power (W)	0.5

Table 6: Constant thruster jet specification

The jet actuator set-up is fairly straightforward. 4 jet actuators have been placed on the -X face of the spacecraft, as shown in table 7 and figure 1. It must be noted that y_0 is a quarter of L_y and z_0 is a quarter of L_z, all taken from the geometric center of the -X face of the spacecraft. L_x, L_y and L_z have been presented in section 4. The inclination is taken with respect to the -Y axis, on the y-z plane.
Thrust is generated on all three axis (even though it will have different magnitudes) because the center of mass is not in the geometric center of the spacecraft, but it is slightly shifted.

[4]M005 Micro Aerospace Solutions: `https://www.micro-a.net/thrusters-tmpl.html`

Identifier	**Location**	**Inclination** [deg]
1	$[-y_0, -z_0]$	-25
2	$[+y_0, -z_0]$	-155
3	$[+y_0, +z_0]$	$+155$
4	$[-y_0, +z_0]$	$+25$

Table 7: Thruster jet orientation

Now the final jet thruster matrix can be written. It has as many columns as number of jets (which is 4 for this case) and 3 rows, one for each direction.

$$T_{thr} = \begin{bmatrix} -0.4391 & 1.0730 & 0.2864 & -0.9204 \\ -3.4866 & -3.4866 & 3.4866 & 3.4866 \\ 7.4770 & -7.4770 & -7.4770 & 7.4770 \end{bmatrix} 10^{-4} \text{ Nm} \tag{12}$$

At each time step, a minimization problem has to be solved to decide which actuators must be used. Since all the actuators are either on or off, only 16 configurations are possible. The formula is:

$$\mathbf{T}_p = min\left(|\mathbf{T}_c - T_{thr}\mathbf{u}_i|\right) \tag{13}$$

where $\mathbf{T}_p$ is the torque output by the jets at each time step, $\mathbf{T}_c$ is the torque coming from the control block and $\mathbf{u}_i$ is a column vector of 4 elements and each elements corresponds to a jet, each element can be either 0 or 1 (for off or on). In the jets model, the program simply cycles through all 16 possibilities of $\mathbf{u}_i$ and chooses the one which follows the relationship 13 shown above. This is faster than implementing a proper minimization algorithm as the possibilities are very limited.

6.2 Reaction wheels

The other actuator type which has been implemented is reaction wheels. For this mission, 4 of them have been implemented in a pyramidal configuration. The specifications for the reaction wheels have been recovered from NanoAvionics[5], as shown in table 7:

Max torque [Nm]	0.0032
Max momentum storage [Nms]	0.020
Power consumation peak [W]	3.250
Mass [kg]	0.137
Dimensions [mm]	43.5 x 43.5 x 24

Table 8: Reaction wheel specifications

Whenever the reaction wheels are saturated, an algorithm will de-saturate them by making use of the constant jet thrusters. Then, the stored angular momentum is obtained by integrating:

$$\dot{\mathbf{h}}_{RW} = -A^*_{RW}\left(\mathbf{T}_c + \boldsymbol{\omega} \times I\boldsymbol{\omega} + \boldsymbol{\omega} \times A_{RW}\mathbf{h}_{RW}\right) \tag{14}$$

where:

$$A_{RW} = \frac{1}{\sqrt{3}} \begin{bmatrix} -1 & 1 & 1 & -1 \\ -1 & -1 & 1 & 1 \\ 1 & 1 & 1 & 1 \end{bmatrix} \quad \text{and} \quad A^*_{RW} = \frac{\sqrt{3}}{4} \begin{bmatrix} -1 & -1 & 1 \\ 1 & -1 & 1 \\ 1 & 1 & 1 \\ -1 & 1 & 1 \end{bmatrix}$$

[5] 4RW NanoAvionics: `https://nanoavionics.com/CubeSAT-components/`

During the de-saturation phase the thrusters have to provide both the de-saturation torque and the control torque. The total required torque $\mathbf{T}_d$ is:

$$\mathbf{T}_d = \mathbf{T}_c + A_{RW}\mathbf{h}_{RW} \tag{15}$$

$\mathbf{T}_d$ is used to compute the real torque of thrusters $\mathbf{T}_t$. Finally, the de-saturation term must be subtracted to obtain the provided control torque $\mathbf{T}_p$

$$\mathbf{T}_p = \mathbf{T}_t - A_{RW}\mathbf{h}_{RW} \tag{16}$$

7 Perturbation Torques

Along his orbit the spacecraft is affected by environment forces i.e. torques due to:

Atmospheric Drag (AD): Usually, the AD has a higher impact when the spacecraft is at the pericenter of its orbit, because of the large speeds and low altitudes.

Gravity Gradient (GG): The GG is usually impactful for a larger sized spacecraft than a CubeSAT, so it's quite plausible that for this mission the resulting torque will be very small.

Magnetic Field (MF): Since this satellite will operate in LEO, a large contribution of the MF is expected.

Solar Radiation Pressure (SRP): SRP is known as the most relevant cause of perturbation in deep space. Conversely, in LEO it should occupy a secondary role but not straightway negligible.

7.1 AD Torque

The aerodynamic drag torque is given by:

$$\mathbf{T}_{AD} = \begin{cases} -\frac{1}{2} c_d \, \rho \, v_r^2 \sum_{i=1}^{n} \mathbf{r}_i \times \frac{\mathbf{v_r}}{||\mathbf{v_r}||} \sum_{i=1}^{n} \left(\mathbf{n}_i \cdot \frac{\mathbf{v_r}}{||\mathbf{v_r}||} \right) A_i & \text{if } \mathbf{n}_i \cdot \frac{\mathbf{v_r}}{||\mathbf{v_r}||} > 0 \\ 0 & \text{otherwise} \end{cases} \tag{17}$$

Once the shape of the spacecraft is fixed, the drag coefficient c_d and areas A_i, as well as their normal orientation $\mathbf{n}_i$ and distances with respect to the center of mass $\mathbf{r}_i$ are all given. Drag force is thus proportional to density ρ and to relative velocity square v_r^2. It must be noted that the aerodynamic drag torque is only generated for surfaces exposed to the relative wind.

The density decreases with increasing altitude. At altitude lower than 100 km (Kármán line) the drag grows dramatically wheras on the opposite side, above 1,000 km, drag can be neglected. Table 9 sums up the atmospheric model for Earth's ionosphere, where given an altitude h, the density $\rho(h)$ is estimated interpolating between rows in the table.

$$\rho(h) = \rho(k) \, e^{-\frac{h-h(k)}{H(k)}} \begin{cases} k = \left\lceil \frac{h}{100} \right\rceil & \text{h} \geq 500 \text{ km} \\ k = \left\lceil \frac{h-250}{50} \right\rceil & 250 < \text{h} < 500 \text{ km} \end{cases} \tag{18}$$

The relative velocity $\mathbf{v_r}$ is the spacecraft velocity with respect to the air. The average air

Reference altitude h(k) [km]	**Nominal density ρ(k)** [kg/km^3]	**Scale height H(k)** [km]
250	7.248×10^{-2}	45.546
300	2.418×10^{-2}	53.628
350	9.158×10^{-3}	53.298
400	3.725×10^{-3}	58.515
450	1.585×10^{-3}	60.828
500	6.967×10^{-4}	63.822
600	1.454×10^{-4}	71.835
700	3.614×10^{-5}	88.667
800	1.170×10^{-5}	124.64
900	5.245×10^{-6}	181.05
1000	3.019×10^{-6}	268.00

Table 9: Earth atmospheric model

velocity is due to Earth rotation. In addiction, gusts of air random contributions at 300 km/h can be taken into account. The air velocity in ECI is:

$$\mathbf{v}_{air} = \boldsymbol{\omega}_{earth} \times \mathbf{r}_{xy} + \mathbf{v}_{gusts} \tag{19}$$

where:

- $\boldsymbol{\omega}_E = \left[0,\ 0,\ \dfrac{2\pi}{T_{day}}\right]^T$ with $T_{day} = 86164.1$ s
- $\mathbf{r}_{xy} = [r_x,\ r_y,\ 0]^T$ which are the x and y coordinates of the spacecraft orbit radius

7.2 GG Torque

Let's define the radius $\mathbf{r}$ from Earth to spacecraft CoM in BODY frame coordinates such that:

$$\mathbf{r} = r(c_1, c_2, c_3) \tag{20}$$

The GG torque is given by:

$$\begin{cases} T_{GG,x} = -3\dfrac{\mu}{r^3}(I_y - I_z)c_2c_3 \\ T_{GG,y} = -3\dfrac{\mu}{r^3}(I_z - I_x)c_1c_3 \\ T_{GG,z} = -3\dfrac{\mu}{r^3}(I_x - I_y)c_1c_2 \end{cases} \tag{21}$$

Note that the GG torque is inversely proportional to the third power of the distance from the attractor (Earth) and directly proportional to inertia differences.

7.3 MF torque

The Earth magnetic field can be modelled by:

$$b_r = \sum_{n=1}^{k} \left(\frac{R}{r}\right)^{n+2} (n+1) \sum_{m=0}^{n} (g_n^m \cos m\phi + h_n^m \sin m\phi) P_n^m(\theta) \tag{22}$$

$$b_\theta = -\sum_{n=1}^{k} \left(\frac{R}{r}\right)^{n+2} \sum_{m=0}^{n} (g_n^m \cos m\phi + h_n^m \sin m\phi) \frac{\delta P_n^m(\theta)}{\delta\theta} \tag{23}$$

$$b_\phi = -\frac{1}{sin\theta} \sum_{n=1}^{k} \left(\frac{R}{r}\right)^{n+2} \sum_{m=0}^{n} (-g_n^m \sin m\phi + h_n^m \cos m\phi) P_n^m(\theta) \tag{24}$$

- R is the Earth's equatorial radius.
- r, θ and ϕ are the spherical coordinates of the position of the satellite: distance from the center of the Earth, colatitude and East longitude from Greenwich
- The gaussian coefficients g_n^m and h_n^m are known by IGRF tables up to order k.
- P_n^m is computed by polynomial recursive formula ([1])

Knowing the spacecraft declination δ and right ascension α, the magnetic field $\mathbf{B}$ is transformed in ECI coordinates.

$$b_1 = (b_r \cos\delta + b_\theta \sin\delta)\cos\alpha - b_\phi \sin\alpha \tag{25}$$

$$b_2 = (b_r \cos\delta + b_\theta \sin\delta)\sin\alpha + b_\phi \cos\alpha \tag{26}$$

$$b_3 = b_r \sin\delta - b_\theta \cos\delta \tag{27}$$

Finally, the magnetic torque is computed in BODY frame:

$$\mathbf{T}_{MF} = \mathbf{m} \times (A_{B/N}\mathbf{b}) \tag{28}$$

7.4 SRP torque

The average solar pressure at 1 AU is known:

$$P = \frac{F_{1AU}}{c} \tag{29}$$

where:

- $F_{1AU} = 1358 \frac{W}{m^2}$ is the average solar radiation pressure at Earth's surface.
- $c = 2.99792 \times 10^8 \frac{m}{s}$ is the light speed.

Then, the torque is:

$$\mathbf{T}_{SRP} = \sum_{i=1}^{n} \mathbf{r}_i \times \mathbf{F}_i \tag{30}$$

$$\mathbf{F}_i = \begin{cases} -PA_i \left(\mathbf{s}_b \cdot \mathbf{n}_i\right) \left[(1-\rho_{s,i})\mathbf{s}_b + \left(2\rho_{s,i}\left(\mathbf{s}_b \cdot \mathbf{n}_i\right) + \frac{2}{3}\rho_{d,i}\right)\mathbf{n}_i\right] & \text{if } \mathbf{s}_b \cdot \mathbf{n}_i > 0 \\ 0 & \text{otherwise} \end{cases} \tag{31}$$

where:

- $\mathbf{n}_i$ is the normal orientation of the i^{th} surface, with area A_i.
- $\rho_{s,i}, \rho_{d,i}$ are scattering and dispersion indices of the i^{th} surface.
- $\mathbf{s}_b$ is the unit vector pointing the Sun in BODY frame.
- $\mathbf{r}_i$ is the vector to the point of application of the force on the i-surface from the CoM.

7.5 Simulation and conclusions

In figure 2 and 3 the magnitude of angular accelerations $\dot{\boldsymbol{\omega}}$ due to disturbance torques is represented. Remember that the attitude subsystem must guarantee two operative phases: Sun-pointing when the spacecraft is exposed to sunlight ($0 < t < 1736$ s $\wedge$ $3944 < t < 5677$ s) and Earth-pointing while the spacecraft is in eclipse ($1737 < t < 3943$ s).

- $\dot{\boldsymbol{\omega}}_{AD}$: AD is higher during the Sun-pointing phase since the spacecraft orbit is closer to its pericenter, which means the height is the lowest and the solar panels are oriented towards the relative wind. However during the Earth-pointing phase, the AD drastically decreases because the exposed surface to the relative wind decreases, the air density decreases and the relative velocity decreases as well.
- $\dot{\boldsymbol{\omega}}_{GG}$: During the Sun-pointing phase c_2 is almost zero, meaning the y-component of the GG is negligible. During the Earth-pointing phase both c_2, c_3 are close to zero, and therefore GG becomes even smaller since two components are almost negligible.
- $\dot{\boldsymbol{\omega}}_{MF}$: MF fluctuations are due to on-board activity and higher order magnetic field terms. The MF also decreases with altitude, but more slowly then AD and GG. Finally, the MF perturbation is very sensible to how the spacecraft is oriented with respect to the Earth magnetic field (fig.2).
- $\dot{\boldsymbol{\omega}}_{SRP}$: The SRP is more or less constant during the Sun-pointing phase, only depending on the spacecraft orientation, while it's zero in eclipse.

Overall, during the Sun-pointing phase AD plays a dominant role. Instead during Earth-pointing, MF is the only non negligible perturbation.

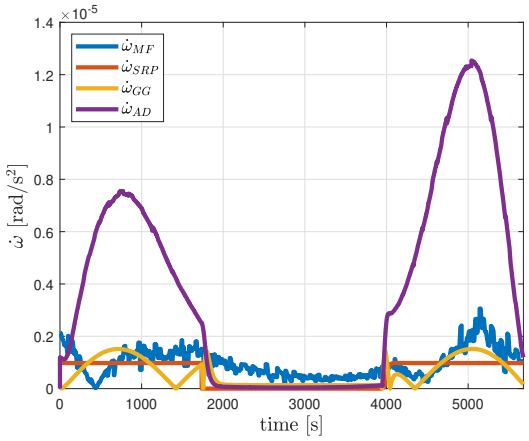

Figure 2: $|\dot{\boldsymbol{\omega}}|$ controlled with RW + Jets

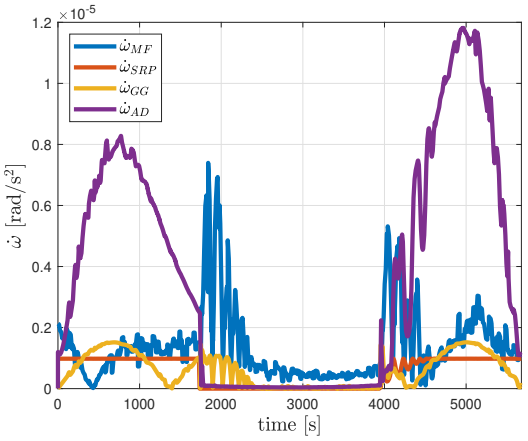

Figure 3: $|\dot{\boldsymbol{\omega}}|$ controlled with Jets

8 Attitude Determination

During regular use (pointing and slew maneuver) the attitude is determined by the Star Sensor by solving Wahba's problem. A check is made at each time step, to make sure the Star Sensor is not facing the Sun. If this is the case, then only the gyroscope is used for determination of the attitude, by running the obtained $\boldsymbol{\omega}_{gyro}$ inside a kinematic block to find the direct cosine matrix at each step. It must be noted that the during nominal use, the gyroscope will only be used for brief time intervals, therefore its lower accuracy and noisy output of the attitude will not be a problem for the mission.

The two sensors will be switching back and forth, making use of a function that will reset the integration every time the Sun will get inside or outside the field of view of the Star Sensor, by feeding the final condition before the switch as the initial condition of the following integration. Other celestial bodies have not been modelled in this phase. When the Star Sensor is working, it will provide $\mathbf{v}_i^N$ and $\mathbf{s}_i^B$ a each time step. Therefore the attitude is found by solving Wahba's problem analytically, at each time step. It can be shown that solving Wahba's problem is the same as maximizing the B matrix, defined as:

$$B = \frac{1}{3}\sum_{i=1}^{3} \mathbf{v}_i^N \mathbf{s}_i^B \tag{32}$$

It must be noted that since the measurements strictly come from the Star Sensor, the weight of each measurement must be the same, and since 3 stars are used, the weight has to be set to 1 third. Then, the attitude direct cosine matrix can be recovered by decomposing B using singular value decomposition, so that $B = U\Sigma^T V^T$, and finally:

$$\tilde{A}_{B/N} = U \begin{bmatrix} 1 & 0 & 0 \\ 1 & 1 & 0 \\ 0 & 0 & det(U)det(V) \end{bmatrix} V^T \tag{33}$$

It must be noted that during detumbling, the attitude will not be calculated. This is due to the fact that the driving parameter for this phase of the mission is the angular velocity of the spacecraft, and its orientation is not of interest (at least for now) since only the gyroscope will be used. All this will be explained more in detail in section 9.1.

9 Attitude Control

9.1 Detumbling

Detumbling is the first phase of the mission. The objective is to minimize $|\omega|$ starting from a random initial condition, within a reasonable amount of time. The detumbling maneuver is obtained by only making use of the gyroscope and the thrusters, which are those given by the project specifications. The decision has been not to add any other sensor or actuator for the detumbling, as it is generally a low-requirement phase of the mission, and regardless, decent results can be obtained with this architecture. First of all, the starting angular velocity has been set to $\boldsymbol{\omega}_0 = [12, -9, -11]$ which is a reasonable initial value. Two distinct phases are used to accomplish the goal for the detumbling.

The first phase is the rougher, but also computationally quicker. A proportional law is used to find the torque necessary to perform the maneuver.

$$\mathbf{T}_c = -\mathbf{k}_{\omega_1} \boldsymbol{\omega}_{gyro} \tag{34}$$

where $\boldsymbol{\omega}_{gyro}$ comes from eq. 7, and the parameters $\mathbf{k}_\omega$ have been set as $[1,\ 1/4,\ 1/16] \times 0.8$. This phase lasts for 2500 seconds, enough for $||\boldsymbol{\omega}||$ to reach values smaller than 1 degree per second (or 0.018 radians per second). This type of control alone is not able to reach for smaller values of $||\boldsymbol{\omega}||$ due to the noise coming from the gyroscope.

Therefore, a second phase of de-tumbling is used. An extended observer is implemented, to estimate the angular velocity and any disturb acting on the system.

$$\begin{cases} \dot{\boldsymbol{\omega}}_{est} & = I^{-1}\left(I\boldsymbol{\omega} \times \boldsymbol{\omega} + \mathbf{T}_{pert} + \mathbf{T}_p\right) + k_a\left(\boldsymbol{\omega}_{gyro} - \boldsymbol{\omega}_{est}\right) \\ \dot{\mathbf{d}}_{est} & = k_b\left(\boldsymbol{\omega}_{gyro} - \boldsymbol{\omega}_{est}\right) \end{cases} \tag{35}$$

The parameters k_a and k_b have respectively been set to 0.05 and 0.005. The control law becomes:

$$\mathbf{T}_c = -\mathbf{k}_{\omega_2}\boldsymbol{\omega}_{est} - \mathbf{d}_{est} \tag{36}$$

and in this case $\mathbf{k}_{\omega_2}$ has been set to $[1/2,\ 1/2,\ 1] \times 0.6$. This phase only lasts for 60 seconds, but it is enough to decrease the value of $||\boldsymbol{\omega}||$ down to around 0.03 degrees per second (or 5×10^{-4} radians per second). All the results are shown in figures 4, 5, 6 and 7, displaying the time evolution of the true angular velocities $\boldsymbol{\omega}$, the true direction cosine matrix A_{ij} and the jet thruster command vector $\mathbf{u}_i$. In the case of $\boldsymbol{\omega}$ and A_{ij}, only the most relevant part is shown, from t = 2000 s onward.

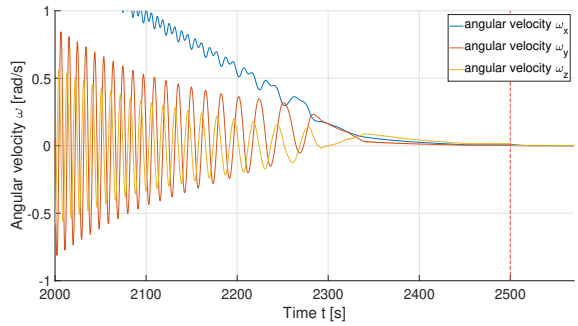

Figure 4: $\boldsymbol{\omega}$ during de-tumbling

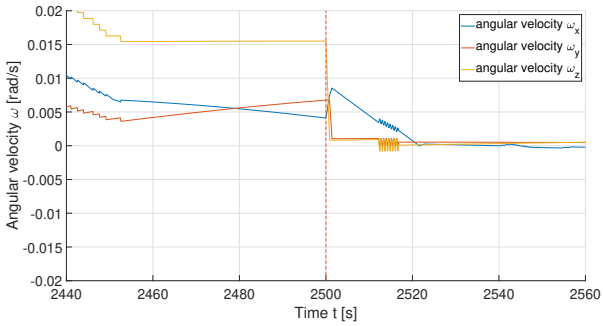

Figure 5: $\boldsymbol{\omega}$ during de-tumbling, zoom

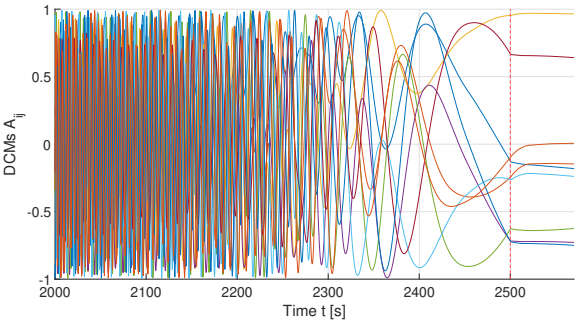

Figure 6: A_{ij} during de-tumbling

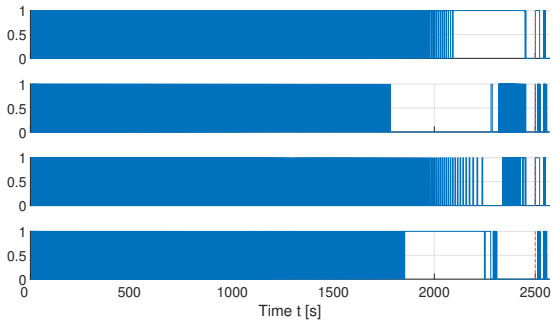

Figure 7: $\mathbf{u}_i$ during de-tumbling

Both phases have been bounded in order to avoid excessive fuel consumption:

- 1^{st} phase: if $||\boldsymbol{\omega}_{gyro}|| < 0.02\ \frac{rad}{s}$, then $\mathbf{T}_p = [0,0,0]^T$
- 2^{nd} phase: if $||\boldsymbol{\omega}_{est}|| < 0.0007\ \frac{rad}{s}$, then $\mathbf{T}_p = [0,0,0]^T$

which means that whenever the driving parameter (either $||\boldsymbol{\omega}_{gyro}||$ or $||\boldsymbol{\omega}_{est}||$) becomes too small, then the actuators will be shut off. If the actuators were not bounded, they would not be able to stop the motion below a certain threshold, and could only transfer the kinetic energy from an axis to another, resulting in oscillatory behaviour and overall waste of propellant mass, which is why these boundaries have been put in place.

9.2 Slew maneuver

9.3 Pointing

The esteemed attitude error cosine matrix $\tilde{A}_e$ is given by the esteemed body attitude $\tilde{A}_{B/N}$ and the target attitude $A_{T/N}$:

$$\tilde{A}_e = \tilde{A}_{B/N} A_{T/N}^T = \begin{bmatrix} a_{11} & a_{12} & a_{13} \\ a_{21} & a_{22} & a_{23} \\ a_{31} & a_{32} & a_{33} \end{bmatrix} \tag{37}$$

where $A_{T/N}$ is either equal to $A_{L/N}$ during the Earth-pointing phase (eq. 4), or to $A_{S/N}$ during the Sun-pointing phase (eq. 5). The control torque $\mathbf{T}_c$ function is:

$$\mathbf{T}_c = \begin{cases} T_{c,x} = -k_{p,x}\alpha_x - k_{d,x}(\omega_x - \bar{\omega}_x) \\ T_{c,y} = -k_{p,y}\alpha_y - k_{d,y}(\omega_z - \bar{\omega}_y) \\ T_{c,z} = -k_{p,z}\alpha_z - k_{d,z}(\omega_z - \bar{\omega}_z) \end{cases} \tag{38}$$

where:

$$\boldsymbol{\alpha} = \left[\frac{a_{23} - a_{32}}{2}, \frac{a_{31} - a_{13}}{2}, \frac{a_{12} - a_{21}}{2} \right]^T \quad \text{and} \quad \bar{\boldsymbol{\omega}} = \begin{cases} \left[0, \sqrt{\frac{\mu}{r^3}}, 0\right]^T & \text{if Earth-pointing} \\ \left[0, \frac{2\pi}{T_{year}}, 0\right]^T & \text{if Sun-pointing} \end{cases}$$

The parameters k_p, k_d have been set to:

$$k_p = 0.016 \left[\frac{I_x}{I_z}, \frac{I_y}{I_z}, 1 \right]^T \qquad k_d = 0.072 \left[\frac{I_x}{I_z}, \frac{I_y}{I_z}, 1 \right]^T \quad \text{for thruster jets}$$

$$k_p = 0.0016 \left[\frac{I_x}{I_z}, \frac{I_y}{I_z}, 1 \right]^T \qquad k_d = 0.0072 \left[\frac{I_x}{I_z}, \frac{I_y}{I_z}, 1 \right]^T \quad \text{for reaction wheels}$$

The control torque $\mathbf{T}_c$ is bounded, in order to flatten the peaks:

$$\mathbf{T}_c \in \pm 10^{-2} \left[\frac{I_x}{I_z}, \frac{I_y}{I_z}, 1 \right]^T \quad \text{for thruster jets}$$

$$\mathbf{T}_c \in \pm 10^{-3} \left[\frac{I_x}{I_z}, \frac{I_y}{I_z}, 1 \right]^T \quad \text{for reaction wheels}$$

and it is filtered to zero when its norm is smaller than 10^{-6} Nm.

Once the control torque $\mathbf{T}_c$ is computed, the actuators have to provide it as accurately as possible. In figure 8 the performances are plotted: there are some isolated peaks due to attitude determination; other long-term and marked oscillations are related to the transition to switch the phase from Earth to Sun pointing and vice versa; Overall, the error angle $\boldsymbol{\alpha}$ is bounded. Unfortunately, in this configuration 12.9 g propellant are required for each orbit as shown in figure 9. If this number is multiplied by 90 days, which could be reasonable number of days for a short term mission, the total propellant mass required would be of 17.67 kg, which is clearly unfeasible. This is the reason why reaction wheels have been added in order to keep the amount of fuel required for the mission under control, as well as improving the accuracy for the pointing.

The new simulation, plotted in figure 10 and 11 shows an improvement in performances, since the error angle $\boldsymbol{\alpha}$ is smaller then before, as expected. The solution is feasible, as the stored angular momentum $\mathbf{h}$ is significantly less than the maximum listed in the reaction wheel datasheet. Note that the reaction wheels are sized so that de-saturation is not strictly required at each orbit, however the decision has been to implement a preventive strategy, and have a de-saturation maneuver performed at the pericenter of every orbit, lasting 5 seconds, in order to avoid any issue at the cost of a slightly higher propellant mass usage. The resulting propellant mass requirement is slightly less than 0.035 g each orbit, and therefore a theoretical 90 days mission would only require 47.86 g of propellant mass.

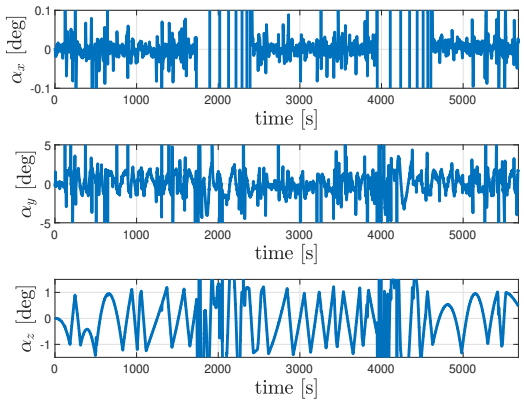

Figure 8: Error angle $\boldsymbol{\alpha}$ - without RWs

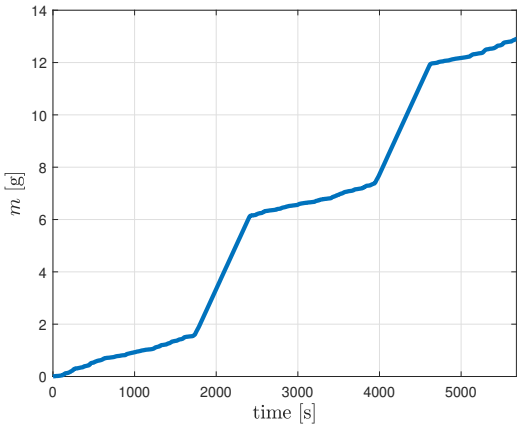

Figure 9: Propellant mass m - without RWs

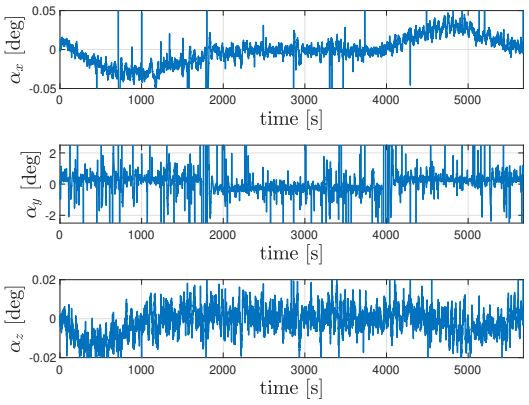

Figure 10: Error angle $\boldsymbol{\alpha}$ - with RWs

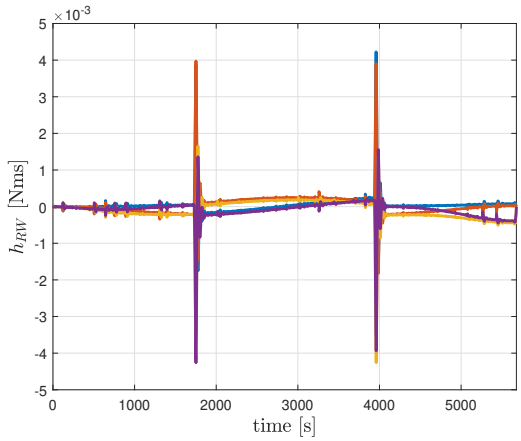

Figure 11: Stored angular momentum $\mathbf{h}_{RW}$ - with RWs

10 Conclusions

11 Bibliography

References

[1] F. Bernelli Zazzara. *Course notes. Spacecraft Attitude Dynamics*. Politecnico di Milano, 2022.